






Dynamic magnetic properties of amorphous $\text{Fe}_{80}\text{B}_{20}$ thin films and their relation to interfaces

Cite as: AIP Advances **10**, 015013 (2020); <https://doi.org/10.1063/1.5129996>

Submitted: 21 October 2019 . Accepted: 05 December 2019 . Published Online: 07 January 2020

U. Urdirroz, B. M. S. Teixeira , F. J. Palomares , J. M. Gonzalez , N. A. Sobolev , F. Cebollada , and A. Mayoral

COLLECTIONS

Paper published as part of the special topic on [64th Annual Conference on Magnetism and Magnetic Materials](#), [Chemical Physics](#), [Energy, Fluids and Plasmas](#), [Materials Science](#) and [Mathematical Physics](#)



View Online



Export Citation



CrossMark

ARTICLES YOU MAY BE INTERESTED IN

[Spin wave modulation by topographical perturbation in \$\text{Y}_3\text{Fe}_5\text{O}_{12}\$ thin films](#)

AIP Advances **10**, 015015 (2020); <https://doi.org/10.1063/1.5130186>

[Magnetization reversal mechanisms in Fe/NiO bilayers grown onto nanoporous alumina membranes and Si wafers](#)

AIP Advances **10**, 015113 (2020); <https://doi.org/10.1063/1.5130172>

[Introduction to antiferromagnetic magnons](#)

Journal of Applied Physics **126**, 151101 (2019); <https://doi.org/10.1063/1.5109132>

AIP Advances

Nanoscience Collection

READ NOW!

Dynamic magnetic properties of amorphous Fe₈₀B₂₀ thin films and their relation to interfaces

Cite as: AIP Advances 10, 015013 (2020); doi: 10.1063/1.5129996

Presented: 6 November 2019 • Submitted: 21 October 2019 •

Accepted: 5 December 2019 • Published Online: 7 January 2020



U. Urdiroz,^{1,2} B. M. S. Teixeira,³ F. J. Palomares,¹ J. M. Gonzalez,¹ N. A. Sobolev,^{3,4} F. Cebollada,^{2,a)} and A. Mayoral⁵

AFFILIATIONS

¹Instituto de Ciencia de Materiales de Madrid (CSIC), Sor Juana Inés de la Cruz, 3, 28049 Madrid, Spain

²POEMMA-CEMDATIC, ETSI de Telecomunicación, Universidad Politécnica de Madrid, 28040 Madrid, Spain

³Departamento de Física and I3N, Universidade de Aveiro, 3810-193 Aveiro, Portugal

⁴National University of Science and Technology "MISIS", 119049 Moscow, Russia

⁵Advanced Microscopy Laboratory - Nanoscience Institute of Aragon (LMA-INA), Mariano Esquillor, s/n, 50018 Zaragoza, Spain

Note: This paper was presented at the 64th Annual Conference on Magnetism and Magnetic Materials.

a) Corresponding author: Federico cebollada, e-mail: fcebollada@etsit.upm.es

ABSTRACT

We present a ferromagnetic resonance study of the dynamic properties of a set of amorphous Fe-B films deposited on Corning Glass[®] and MgO (001) substrates, either with or without capping. We show that the in plane anisotropy of the MgO grown films contains both uniaxial and biaxial components whereas it is just uniaxial for those grown on glass. The angular dependence of the linewidth strongly differs in terms of symmetry and magnitude depending on the substrate and capping. We discuss the role of the interfaces on the magnetization damping and the generation of the anisotropy. We obtained values of the intrinsic damping parameters comparable to the lowest ones reported for amorphous films of similar compositions.

© 2020 Author(s). All article content, except where otherwise noted, is licensed under a Creative Commons Attribution (CC BY) license (<http://creativecommons.org/licenses/by/4.0/>). <https://doi.org/10.1063/1.5129996>

INTRODUCTION

Designing magnetic materials for high frequency applications is crucial for emerging magnetic technologies such as spintronics and magnonics.^{1,2} Relevant to those applications is understanding the magnetization relaxation mechanisms of thin films. The damping parameter α in the Landau-Lifshitz-Gilbert (LLG) equation is directly related to the ferromagnetic resonance (fmr) peaks' linewidth $\Delta H = \Delta H_o + \Delta H_m + \Delta H_G + \Delta H_{TMS}$.³ The first two terms, frequency independent, correspond to inhomogeneities (ΔH_o) and mosaicity (ΔH_m); the isotropic, intrinsic Gilbert term ΔH_G results from the energy transfer from magnetization to lattice; finally, ΔH_{TMS} gives the "two magnon scattering" (TMS), due to the energy transfer from the fmr uniform mode (wavevector $\vec{k}=0$) to degenerate magnons with $\vec{k}\neq 0$.⁴⁻⁸ Many works have analyzed the role of the structure on the damping in magnetic films. Studies of the effects of interfaces, dislocation networks or specific surface

features provide examples of the extrinsic character of the relaxation mechanisms.⁹⁻¹¹ Until recently, little attention has been paid to the damping mechanisms of amorphous transition metal-metalloid thin films,¹²⁻¹⁴ which are good candidates for low damping materials due to their homogeneity and to the possibility of tailoring their magnetic properties by thermal treatments.¹⁵ In this paper we study the dynamic magnetic properties of amorphous Fe₈₀B₂₀ alloys deposited on Corning Glass[®] and MgO (001) substrates, either Au capped or uncapped.

EXPERIMENTAL

Amorphous Fe₈₀B₂₀ thin films were grown by means of a Nd-YAG Pulsed Laser Deposition (PLD) system ($\lambda=532$ nm, 4 ns pulses of 180 mJ, 10 Hz rate), under ultrahigh vacuum conditions. Two films, 20 nm thick, were deposited on square 5x5 mm² Corning Glass[®] substrates, one of them uncapped (C0), the other capped

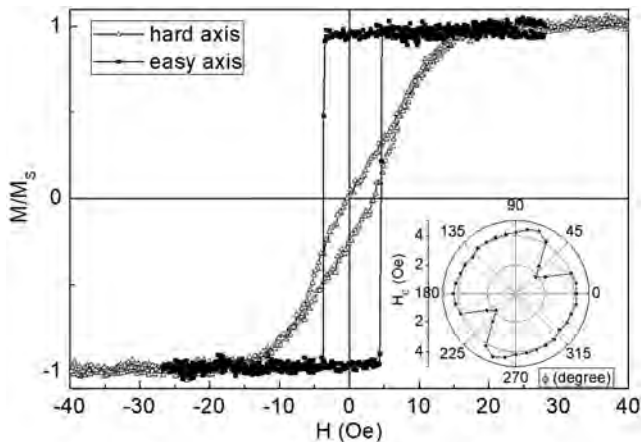


FIG. 1. Easy and hard axis loops of the MAU film; angular dependence of its coercivity (inset).

with a 7 nm Au layer (CAu). Another two films with the same thickness were deposited on MgO (001) substrates with the same dimensions, one uncapped (M0), the other capped with a 7 nm Au layer (MAu). Their amorphicity was checked by X-ray diffraction (XRD) using an 8 circles Bruker diffractometer and Transmission Electron Microscopy (TEM), using a FEI TITAN low base and a FEI high resolution TITAN. Their magnetic hysteresis was studied by transverse magneto-optic Kerr effect (MOKE), under maximum applied fields of 0.5 T. A Bruker E-500 electron paramagnetic resonance spectrometer (X-band, $f = 9.87$ GHz) was employed to study their magnetization dynamics, through the in-plane (IP) angular dependence of the fmr spectra down from saturation at 1.4 T, obtained measuring the

derivative of the imaginary part of the dynamic susceptibility in a Lock-in arrangement.

RESULTS AND DISCUSSION

Figure 1 presents two hysteresis loops measured in the MAU film with the applied field parallel to each diagonal of the substrate. One of the loops is square, with a coercivity close to 5 Oe and a reduced remanence approximately equal to 1, corresponding to a magnetic easy axis (e.a). A magnetization rotation loop is observed along the second diagonal, corresponding to a hard axis (h.a), with little hysteresis and a saturation field of about 15 Oe. The angular evolution of the coercivity (Figure 1, inset) and the remanence show a two-fold, butterfly shape characteristic of uniaxial anisotropy, with minimum values along the h.a. diagonal. All other films present similar features: uniaxial anisotropy with e.a coercivity of a few Oe and h.a. saturation field between 15 and 35 Oe, with the relevant difference that whereas the easy and hard axes of the M films are parallel to the diagonals, those of the C films are parallel to the substrate sides.

The angular dependence of the resonance field H_r (Figures 2(a) and (b)) exhibits two-fold symmetry in all cases. The main differences between the C and the M samples are: (i) the spectra of M films present a single peak along the full angular range and the angular evolution of H_r is not purely symmetric around the maxima and minima; (ii) the spectra of the C films present two overlapping peaks in the angular range 45° - 120° and 225° - 300° , approximately, (Figure 2(a), inset) and the angular dependence of the resonance field is highly symmetric around the maxima and minima. The fits of the resonance field (red lines) to the Smit-Beljers formalism¹⁶ included an IP uniaxial and a cubic anisotropy contribution given by

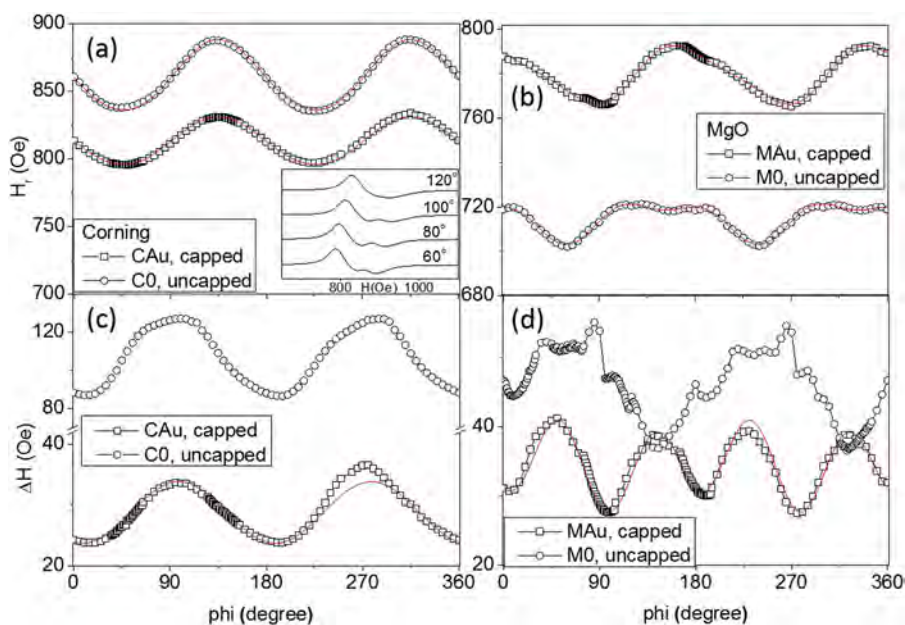


FIG. 2. Angular dependence of the resonance field: C (a) and M (b) films (inset: split peaks measured in C0 at the indicated angles). Angular dependence of the linewidth: C (c) and M (d) films. Red lines: fits indicated in the text.

$$F = \frac{1}{2} \mu_0 M_s^2 \cos^2 \theta - \mu_0 M_s H \sin \theta \cos(\eta - \phi) - k_u \sin^2 \theta \cos^2(\phi - \xi) + \frac{k_c}{4} [\sin^2 2\theta + \sin^4 \theta \sin^2 2\phi] \quad (1)$$

where θ and ϕ are the magnetization polar and azimuthal angles, respectively, K_u (K_c) is the uniaxial (cubic) anisotropy constant, M_s is the spontaneous magnetization, and the cubic (100) and (010) directions are taken as the x and y axes, also respectively. The angles ξ and η , from the x axis, correspond to the uniaxial e.a. and the applied field H direction (both IP). Table I summarizes the fitting parameters and the h.a. saturation field H_{sat} .

As it can be seen, the anisotropy of the C films is purely uniaxial whereas that of the M films has a non-negligible cubic contribution, in addition to the different orientations of the e.a. However, the anisotropy of the M samples is much weaker than that of the C samples. The good agreement between the uniaxial anisotropy field H_{KU} calculated from the anisotropy and the h.a. saturation field is remarkable. The usual sources of anisotropy in amorphous ferromagnets are (i) the magnetoelastic coupling between magnetization and internal stresses, which gives rise to easy (hard) axes in the regions with tensile (compressive) stresses if the magnetostriction is positive, and (ii) the presence of magnetic fields during the fabrication process or annealings. Both produce just uniaxial anisotropies, in no case biaxial anisotropy schemes.¹⁵ The presence of stray fields in our fabrication setup can be ruled out since the different orientations of the axes are not compatible with the identical orientation of all substrates on the sample holder. The anisotropy of Fe-B bulk alloys, about 2 kJm^{-3} , has been calculated from their domain patterns and wall nucleation and pinning magnetization mechanisms.¹⁷ The much lower anisotropy in our films and the well defined orientations of the easy and hard axes are a clear indication of their weak internal stresses (compared to bulk) and, more important, of their spatial homogeneity. The stronger anisotropy of the C films suggests that the stresses induced by the substrate are much stronger than in the M films. Their origin is unclear, a plausible mechanism might be related to the holder-substrate fixation system, which might bend slightly the glass. If the film accommodates to it during the deposition, it will become subjected to the inverse effort after the substrate is relieved from the holder. The weaker anisotropy of the M films indicates that the stresses introduced during the fabrication are lower, probably due to the higher MgO stiffness.

The relevant point is the source of the biaxial component of the anisotropy, which is unusual in amorphous alloys. The TEM studies carried out on an uncapped film deposited on MgO under similar conditions have revealed the formation of a bcc Fe layer,

TABLE I. Fitting parameters from equation (1) and saturation field obtained from the h.a. loops.

Film	K_U (Jm^{-3})	K_C (Jm^{-3})	$\mu_0 M_s$ (T)	H_{KU} (Oe)	H_{KC} (Oe)	H_{sat} (Oe)
C0	1640	-	1.40	29	-	35
CAu	1030	-	1.44	18	-	20
M0	530	260	1.66	8.0	4.0	9
MAu	750	160	1.51	12.4	2.7	13

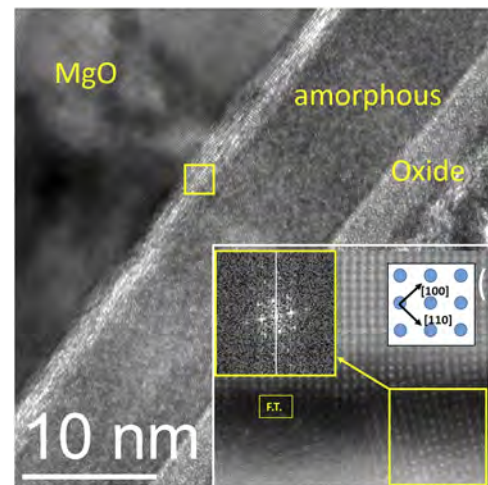


FIG. 3. TEM image of a film deposited on MgO. Inset: high resolution image of the region marked with a yellow square and its Fourier Transform.

about 1 nm thick, at the amorphous-substrate interface and of an oxide layer on the free surface. Figure 3 shows the Fe layer, with a high resolution image (inset) corresponding to the yellow square in the figure. The Fourier transform of this image demonstrates its crystalline nature, the distances calculated for neighboring (100) and (110) planes agreeing with those of bcc Fe, which usually grows epitaxially, with 4% misfit, on MgO (001) with the (100) and (010) axes rotated 45° with respect to those of MgO.¹⁸ The Fe layer can be related to the cubic anisotropy detected by fmr and to the orientation of the uniaxial e.a. along one diagonal. A plausible mechanism for the formation of the e.a. is the orientation of the magnetization of the Fe layer along one of its easy axes during the deposition. The dipolar and/or exchange coupling of the Fe magnetization with that of the layer growing on top of the crystalline layer could act as anisotropy inducing agents. The cubic anisotropy contribution probably results from the interfacial exchange coupling between the Fe layer and film, similar to that occurring in exchange biased systems. The interfacial exchange is likely to extend its influence to the full amorphous layer since its exchange length is of a few tens of nanometers.¹⁹

Up to now, the effect of the Au capping or the free surface oxide has not been discussed. It is evident that it plays no major role in the orientation of the anisotropy axes or the intensity of the internal stresses. In fact, the uncapped C0 film has roughly 50% higher anisotropy than its capped counterpart whereas the anisotropy of the uncapped M0 film is weaker than that of MAu. However, its influence is quite noticeable in the peak linewidth (Figures 2(c) and (d)). Both C0 and CAu films have similar linewidth angular evolution, two-fold with the maxima shifted ca. 45° with respect to the resonance field, where the resonance peak splits. This indicates the presence of a common underlying broadening mechanism. Yet, the magnitude of the linewidth increases in the uncapped sample. The eventual presence of an oxide layer in the uncapped film could be the reason for the large damping increase, likely related to increased inhomogeneities at the amorphous/oxide interface. TMS has been proposed as a source of increased damping in films with linear

structural features.^{6,9,10} Spin waves with wave vector $\vec{k} \neq 0$, \vec{k} perpendicular to the linear structures, appear when the angle between magnetization and \vec{k} is below a critical angle $\phi_C = \arcsin\left[\left(\mu_0 H_0 / B_0\right)^{1/2}\right]$, where H_0 includes the applied and anisotropy fields and $B_0 = \mu_0(H_0 + M_s)$. When the degenerate states can no longer be treated as a perturbation, a resonance peak splitting occurs. We propose the presence of linear tensile stresses parallel to the e.a. as the sole source of anisotropy in the C films. The tensile stresses, taken as linear perturbations with defined orientations, could eventually increase the TMS, leading even to a peak splitting.⁹ However, the critical angle around the perpendicular to the stresses calculated for the C films is roughly $\pm 14^\circ$, much narrower than the measured value. Another plausible explanation might be related to inhomogeneous tensile stresses (variation in their orientation) confined in small regions but large enough to provide separate resonances. The oxide layer of M0 does not increase the linewidth as dramatically as in C0. The complex two-fold structure of the M0 linewidth angular evolution breaks the symmetry of both the uniaxial and biaxial structural features responsible for its anisotropy. In contrast, the MAu linewidth is dominated by a four-fold component, likely related to the Fe layer. The IP angular evolution of the linewidth TMS contribution reproduces the symmetry of the scattering centers, if they centers are linked to the crystal structure, and it can be expressed as a function of the orientation of the crystal axes:^{8,11} The linewidth is then proportional to

$$\alpha_{TMS} = \sum_{X_i} \Gamma_{(X_i)} f(\phi_H - \phi_{(X_i)}) \quad (2)$$

$\Gamma_{(X_i)}$ is the scattering factor along the main crystal directions and $f(\phi_H - \phi_{(X_i)})$ depends on the applied field direction with respect to them. The linewidth of the capped films can be fitted to an isotropic value ΔH_{iso} plus a function corresponding to equation (2). In the case of amorphous films, those directions could be associated with the internal stress lines and, in MAu, the crystal directions of the Fe interfacial layer. The fits of the CAu and MAu linewidths to ΔH_{iso} plus a function $\Delta H = A \sin^2(\phi_H - \phi_1) + B \sin^2(2(\phi_H - \phi_2))$ (continuous red lines in Figure 2) yield close ΔH_{iso} values (23.5 and 27.5 Oe, respectively) and the following parameters for MAu (CAu): $A=3.5$ (10.1) Oe; $\phi_1=7.4^\circ$ (8.2°); $B=10.8$ Oe; $\phi_2=7.4^\circ$ (no four-fold component in CAu). ΔH_{iso} represents an upper limit of the intrinsic Gilbert Damping, which can be written as^{8,11}

$$\mu_0 \Delta H_{iso} = \Delta H_0 + \alpha \frac{4\pi f}{\gamma} \quad (3)$$

where γ is the gyromagnetic factor (the mosaicity term can be excluded due to the amorphous nature of our films, at least for the C films). The upper limits for the intrinsic damping coefficient α are $3.3 \cdot 10^{-3}$ and $4.0 \cdot 10^{-3}$ for CAu and MAu, respectively, comparable to the lowest values reported for amorphous films of Fe and Fe-Co base.^{12,13,20}

CONCLUSIONS

We studied the role of the film-substrate and film-capping interfaces on the dynamic properties of amorphous Fe-B films. We showed that the films deposited on glass present stronger IP

anisotropy than those deposited on MgO (001), probably due to higher residual stresses, and that the formation of a thin Fe layer on MgO induces a four-fold anisotropy, not usual in amorphous alloys. The damping of the uncapped films is increased due to the oxide layer on top. The damping of the capped samples can be interpreted as a combination of an isotropic and an angle dependent contribution, probably related to TMS. The role of the linear stresses in the amorphous phase and of the exchange Fe-FeB in the MgO/FeB/Au film was discussed.

ACKNOWLEDGMENTS

We thank the financial support by Spanish MINECO, Grant Nos. MAT2013-47878-C2-R and MAT2016-80394-R. U.U. acknowledges FPI grant BES-2014-070387. B.M.S.T. and N.A.S. acknowledge financial support of the FCT of Portugal through the Project No. I3N/FSCOSD (Ref. FCT UID/CTM/50025/2019) and through the bursary PD/BD/113944/2015. N.A.S. was supported by the Ministry of Education and Science of the Russian Federation in the framework of the Increase Competitiveness Program of NUST "MISI" (no. K2-2019-015).

REFERENCES

- C. Chappert, A. Fert, and F. N. V. Dau, *Nat. Mater.* **6**, 813 (2007).
- V. V. Kruglyak, S. O. Demokritov, and D. Grundler, *J. Phys. D Appl. Phys.* **43**, 264001 (2010).
- S. Akansel, A. Kumar, N. Behera, S. Husain, R. Brucas, S. Chaudhary, and P. Svedlindh, *Phys. Rev. B* **97**, 134421 (2018).
- R. Arias and D. L. Mills, *Phys. Rev. B* **60**, 7395 (1999).
- D. L. Mills and S. M. Rezende, in *Spin Dynamics in Confined Magnetic Structures II*, (B. Hillebrands and K. Ounadjela eds.) Topics in Appl. Phys. **87**, 27 (2003).
- R. Arias and D. L. Mills, *J. Appl. Phys.* **87**, 5455 (2000).
- Kh. Zakeri, J. Lindner, I. Barsukov, R. Meckenstock, M. Farle, U. von Hörsten, H. Wende, W. Keune, J. Rucker, S. S. Kalarickal, K. Lenz, W. Kuch, K. Baberschke, and Z. Frait, *Phys. Rev. B* **76**, 104416 (2007).
- A. Conca, S. Keller, M. R. Schweizer, E. Th. Papaioannou, and B. Hillebrands, *Phys. Rev. B* **98**, 214439 (2018).
- R. D. McMichael, D. J. Twisselmann, J. E. Bonevich, A. P. Chen, and W. F. Egelhoff, Jr., *J. Appl. Phys.* **91**, 8647 (2002).
- M. Körner, K. Lenz, R. A. Gallardo, M. Fritzsche, A. Mücklich, S. Facsko, J. Lindner, P. Landeros, and J. Fassbender, *Phys. Rev. B* **88**, 054405 (2013).
- G. Woltersdorf and B. Heinrich, *Phys. Rev. B* **69**, 184417 (2004).
- M. Konoto, H. Imamura, T. Taniguchi, K. Yakushiji, H. Kubota, A. Fukushima, K. Ando, and S. Yuasa, *Appl. Phys. Express* **6**, 073002 (2013).
- M. Bersweiler, H. Sato, and H. Ohno, *IEEE Mag. Lett.* **8**, 1 (2017).
- J. Wang, C. Dong, Y. Wei, X. Lin, B. Athey, Y. Chen, A. Winter, G. M. Stephen, D. Heiman, Y. He, H. Chen, X. Liang, C. Yu, Y. Zhang, E. J. Podlaha-Murphy, M. Zhu, X. Wang, J. Ni, M. McConney, J. Jones, M. Page, K. Mahalingam, and N. X. Sun, *Phys. Rev. Applied* **12**, 034011 (2019).
- T. Egami, *Rep. Prog. Phys.* **47**, 1601 (1984).
- J. Smit and H. G. Beljers, *Philips Res. Rep.* **10**, 113 (1955).
- G. Schroeder, R. Schäfer, and H. Kronmüller, *Phys. Stat. Sol. A* **50**, 475 (1978).
- E. Paz, F. Cebollada, F. J. Palomares, F. Garcia-Sanchez, and J. M. González, *Nanotechnology* **21**, 255301 (2010).
- J. Stöhr and H. C. Siegmann, *Magnetism* (Springer, Berlin, 2006), p. 514.
- T. Devolder, P.-H. Ducrot, J.-P. Adam, I. Barisic, N. Vernier, J.-V. Kim, B. Ockert, and D. Ravelosona, *Appl. Phys. Lett.* **102**, 022407 (2013).